

## ART-XC: a medium-energy X-ray telescope system for the Spectrum-R-Gamma mission

V. Arefiev<sup>a</sup>, M. Pavlinsky<sup>a</sup>, I. Lapshov<sup>a</sup>, A. Tkachenko<sup>a</sup>, S. Sazonov<sup>ab</sup>, M. Revnivtsev<sup>ab</sup>,  
N. Semena<sup>a</sup>, M. Buntov<sup>a</sup>, A. Vikhlinin<sup>ac</sup>, M. Gubarev<sup>d</sup>, S. O'Dell<sup>d</sup>, B. Ramsey<sup>d</sup>, S. Romaine<sup>c</sup>,  
D. Swartz<sup>e</sup>, M. Weisskopf<sup>d</sup>, G. Hasinger<sup>f</sup>, P. Predehl<sup>f</sup>, S. Grigorovich<sup>g</sup>, D. Litvin<sup>g</sup>,  
N. Meidinger<sup>h</sup>, L. W. Strüder<sup>h</sup>

<sup>a</sup> Space Research Institute, IKI, Moscow, Russia

<sup>b</sup> Max-Planck-Institut für Astrophysik, Garching, Germany

<sup>c</sup> Harvard-Smithsonian Center for Astrophysics, Cambridge, MA, USA

<sup>d</sup> NASA Marshall Space Flight Center, Huntsville, AL, USA

<sup>e</sup> Universities Space Research Association, Huntsville, AL, USA

<sup>f</sup> Max-Planck-Institut für Extraterrestrische Physik, Garching, Germany

<sup>g</sup> The All-Russian Scientific Research Institute for Experimental Physics, VNIIEF, Sarov, Russia

<sup>h</sup> Max-Planck-Institute Semiconductor Laboratory, MPI Halbleiterlabor, Munich, Germany

### ABSTRACT

The ART-XC instrument is an X-ray grazing-incidence telescope system in an ABRIXAS-type optical configuration optimized for the survey observational mode of the Spectrum-RG astrophysical mission which is scheduled to be launched in 2011. ART-XC has two units, each equipped with four identical X-ray multi-shell mirror modules. The optical axes of the individual mirror modules are not parallel but are separated by several degrees to permit the four modules to share a single CCD focal plane detector,  $\frac{1}{4}$  of the area each. The 450-micron-thick pnCCD (similar to the adjacent eROSITA telescope detector) will allow detection of X-ray photons up to 15 keV. The field of view of the individual mirror module is about  $18 \times 18$  arcminutes<sup>2</sup> and the sensitivity of the ART-XC system for 4 years of survey will be better than  $10^{-12}$  erg s<sup>-1</sup> cm<sup>-2</sup> over the 4–12 keV energy band. This will allow the ART-XC instrument to discover several thousand new AGNs.

Keywords: X-ray astrophysical mission, hard X-ray telescope, X-ray mirrors.

### 1. INTRODUCTION

Astronomical Röntgen Telescope (ART-XC) is part of the Spectrum-RG scientific payload. The ART-XC instrument is a medium-energy X-ray telescope system that is optimized for response over the 2–11 keV band. ART-XC complements the softer response of another SRG instrument - the German eROSITA X-ray telescope - allowing the detection of heavily obscured ( $N_{\text{H}} > 3 \times 10^{23}$  cm<sup>-2</sup>) X-ray sources and enhancing the sensitivity of the combined eROSITA+ART instruments in the critical iron-K band by a factor of two, roughly tripling the number of source available for study. The anticipated number of ART-XC detections is 50 000 including about 1 000 heavily-observed AGN in the all-sky survey and a comparable number in deeper wide-field (500 deg<sup>2</sup> total) surveys. During pointed-mode observations, ART-XC will obtain statistically significant spectral data up to 15 keV for bright sources. ART's surveys will provide a minimally-biased nearly-complete census of the local Universe in the 2–11 keV band, detecting all but the most-heavily-observed low-redshift AGN. In the pointed mode, ART complements eROSITA and the contemporaneous hard-X-ray mission NuSTAR by bridging the soft and hard X-ray bands.

The ART-XC would allow the achievement of the following scientific goals:

- Investigate the properties of a large, statistically well-defined sample of AGN, spanning a range of luminosities and redshifts;
- Determine the AGN luminosity function at low  $z$ , fully populating the bright end of the  $\log N - \log S$  distribution and (in conjunction with optical measurements) refining the determination of the local black-hole (BH) mass function;
- Detect local heavily obscured AGN and for the brighter ones study the medium-energy (2–15 keV, including the critical Fe-K band) spectra of very heavily obscured (Compton-thick) sources discovered in other spectral bands;
- Compare the spatial distribution of AGN with the large-scale structure defined by clusters and groups of galaxies, and examine how the extended environment and AGN activity affect each other.

The ART-XC (Figure 1) has two units, each equipped with four identical X-ray multi-shell mirror modules. The optical axes of the individual mirror modules are not parallel but are separated by several degrees to permit the four modules to share a single CCD focal plane detector,  $\frac{1}{4}$  of the area each. The 450-micron-thick pnCCD (similar to the adjacent eROSITA telescope detector) will allow detection of X-ray photons up to 15 keV. The field of view of the individual mirror module is about  $18 \times 18$  arcminutes<sup>2</sup> and the sensitivity of the ART-XC system for 4 years of survey will be better than  $10^{-12}$  erg s<sup>-1</sup> cm<sup>-2</sup> over the 4–12 keV energy band.

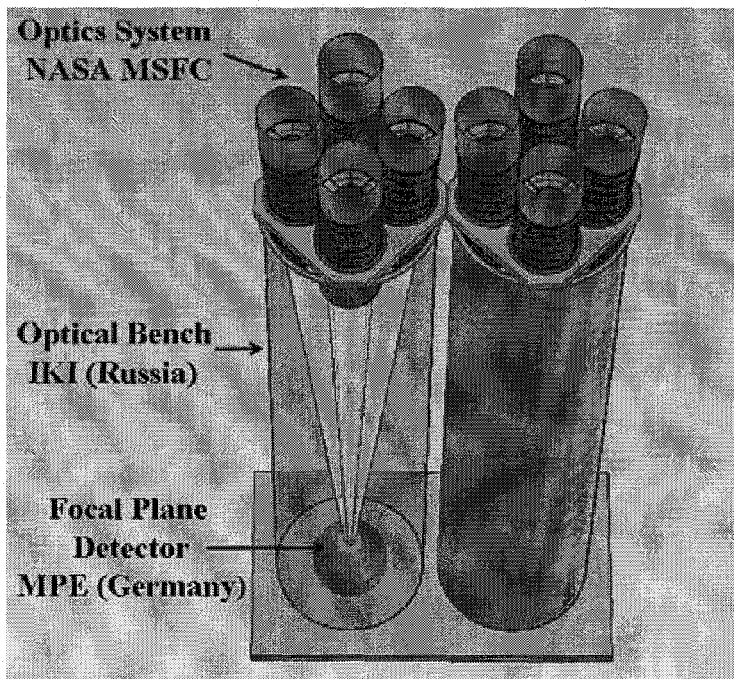


Fig. 1. ART-XC optical scheme with 4 mirror modules looking at slightly different directions to share the same focal plane detector.

## 2. SCIENCE WITH ART-XC

The SRG mission will effectively perform three surveys - the all-sky survey; a 10-times deeper survey near the two Galactic poles; and an even deeper “blank-field” survey during long ( $10^5$  s) pointed observations. Table 1 summarizes the expected results of these surveys, each of which is photon-limited, showing the respective (2–10 keV) sensitivity and number of sources for detection and for rudimentary study ( $> 100$  detected photons) of X-ray spectra and variability.

Table 1: Expected results of the ART-XC 2–10 keV surveys.

ART-XC surveys	Units	All-sky	Polar	Pointed
Survey solid-angle	degree <sup>2</sup>	~41 250	400	125
Detection	erg cm <sup>-2</sup> s <sup>-1</sup>	3.1×10 <sup>-13</sup>	3.4×10 <sup>-14</sup>	8×10 <sup>-15</sup>
	number	52 000	14 000	31 000
Study (> 100 photons)	erg cm <sup>-2</sup> s <sup>-1</sup>	3.8×10 <sup>-12</sup>	4.2×10 <sup>-13</sup>	4.4×10 <sup>-14</sup>
	number	1 000	310	3 100

The SRG eROSITA instrument is more sensitive in the energy band lower than 5 keV in comparison with ART-XC. However, at about 6 keV and above, ART-XC is more sensitive than eROSITA. Therefore, the combination of eROSITA+ART gives the exceptional sensitivity at wide energy band 0.5–10 keV. The harder response of ART relative to eROSITA facilitates the X-ray detection of obscured AGN. Table 2 compares the anticipated number of obscured AGN that the SRG all-sky survey will detect as a function of column density for eROSITA alone, for ART alone, and for eROSITA+ART (combined response). This capability will enable the detection of over a thousand heavily-obscured ( $N_{\text{H}} > 3 \times 10^{23} \text{ cm}^{-2}$ ) AGN, a population that accounts for over half all AGN [1, 2] but has remained elusive even in the deepest X-ray surveys to date [3].

Table 2: Expected detections of heavily obscured AGN during the SRG all-sky survey.

Column $N_{\text{H}}, \times 10^{23} \text{ cm}^{-2}$	eROSITA	ART	eROSITA+ART
>1	5 000	3 000	12 000
>3	600	700	1 800
>10	20	60	100

In addition to the 4-year survey (scanning) phase, the SRG mission plan calls for about 3 years of pointed observations, with expected integration times of 0.1–1 Ms each. Of the 8 ART-XC mirror modules, 1 pair is co-aligned with eROSITA and Calorimeter while the other 3 pairs point several degrees away from the eROSITA direction – which provide for free the blank-field “Pointed” survey (Table 1). The purpose for most of the very deep pointed exposures is to obtain detailed spectra of bright X-ray sources. Thus, while the 6 “off-target” ART-XC modules perform a relatively deep survey, the 2 “on-target” modules will typically accumulate a large number ( $>10^4$ ) counts. For such long exposures on bright non-thermal sources, ART will acquire statistically meaningful data up to about 15 keV.

The SRG observing plan allocates 4 years for the all-sky survey and up to 3 years for pointed observations. During the (scanning) survey phase, ART will image each portion of the sky (in several consecutive orbits) at least every 6 months. For the all-sky survey, the SRG scan axis will undergo controlled precession, resulting in a 200 deg<sup>2</sup> high-exposure area near each orbit pole (Figure 2). The sensitivity of this “polar survey” is nearly an order of magnitude better than the average for the all-sky survey. Many of the same scientific studies to be carried out for the all-sky survey apply to the polar survey. With its deeper exposure, however, the polar survey will extend the science to higher redshifts and thus better address issues of “cosmic evolution”.

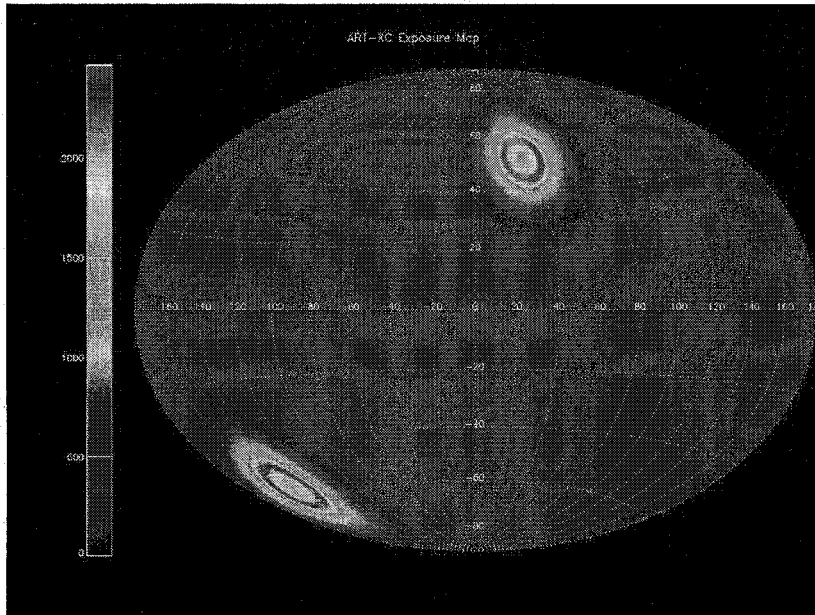


Figure 2: Expected exposure map for a 4-year ART survey shown in galactic coordinates. Each part of the sky will be observed for at least several 100 s and large, 200 deg<sup>2</sup>, regions at high latitude,  $|b| > 40$  deg, will have exposures upwards of 2000 s each.

We estimate that ART, independent of eROSITA, will detect about 50 000 AGN (Table 1) during the all-sky survey, out to a maximum redshift  $z \approx 2$  (Figure 3, left panel). This estimate uses the observed 2–10 keV  $\log N - \log S$  distribution [4] in the appropriate flux range and the energy-dependent ART-XC grasp calculations. Convolving this result with the expected distribution of intrinsic column densities, we estimate that ART-XC will detect many thousands of obscured AGN (Table 2; Figure 3, right panel) including several hundred heavily obscured ( $N_{\text{H}} > 3 \times 10^{23}$  cm<sup>-2</sup>) objects.

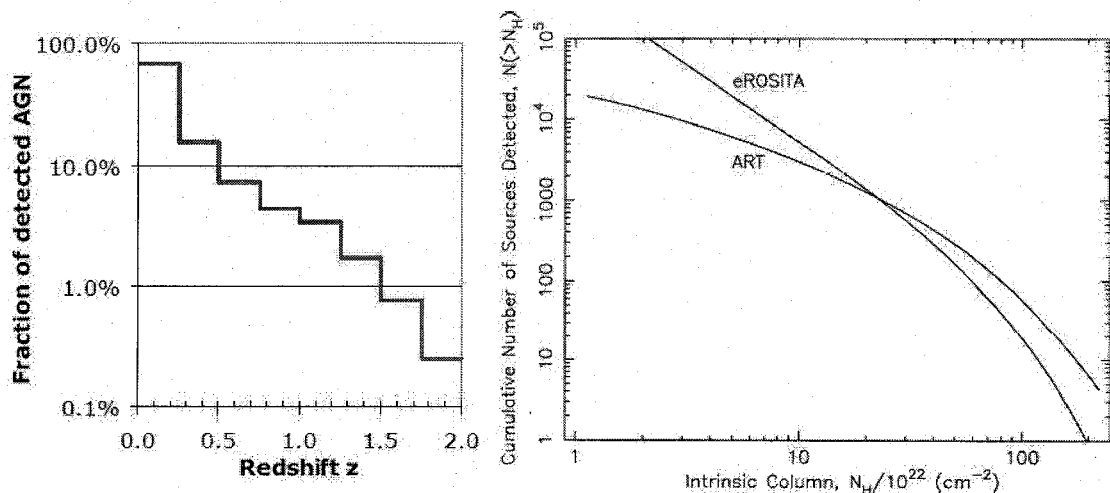


Figure 3: (Left) AGN redshift distribution detected by ART-XC in a 4-year all-sky survey. Approximately following Barger et. al. [5], the AGN luminosity function was assumed to undergo pure luminosity evolution at  $z < 1.2$ , with the characteristic luminosity  $L \sim (1+z)^{3.2}$ , and no evolution afterwards. (Right) Cumulative distribution of AGN detected independently by eROSITA and by ART-XC with column density  $> N_{\text{H}}$ . ART-XC will detect the most heavily obscured AGN that eROSITA will miss.

## 2.1. Obscured AGN

Obscured AGN likely comprise most of the AGN population, provide a major contribution to the cosmic X-ray background, and represent the bulk of the black-hole growth in the Universe. A catalog of heavily absorbed (but not Compton-thick) AGN will be one of the main results of the ART-XC all-sky survey. It will allow a study of the distribution of X-ray absorption column as a function of AGN luminosity [5] and of redshift [6]. In addition, it will constrain AGN unification schemes and the physics of AGN accretion flows. Together with eROSITA and existing deep X-ray surveys (Chandra, XMM-Newton, etc.), ART-XC will make a census of the space density of such objects in the relatively nearby Universe ( $z < 0.3$ ). These data will provide a link to future higher-energy missions that will investigate even more heavily obscured AGN.

## 2.2. High-Luminosity Quasars

The ART-XC survey will also detect representative numbers of the most luminous and rare AGN—quasars. The sensitivity of ART-XC enables the detection of all luminous ( $\approx 10^{46}$  erg  $s^{-1}$ ) quasars out to redshift  $z \approx 1$  (Figure 3, left panel). Such powerful quasars are exceptionally interesting in that they may be the most massive (billions of solar masses) black holes in the making. Thus far only a few tens of such objects have been discovered: They are rare and found only in wide-field surveys. The ART-XC all-sky survey should find hundreds of such objects.

## 2.3. Low-Luminosity AGN

The current census of nearby ( $z < 0.1$ ) active nuclear BHs is limited to relatively bright AGN - Seyfert galaxies with X-ray luminosities  $> 10^{41}$  erg  $s^{-1}$ . However, there are indications that low luminosity AGN (LLAGN) may be present in a significant fraction (perhaps 50%) of nearby galaxies [7]. Moreover, most present-day BH growth may occur at low, substantially subcritical, accretion rates, characterized by low radiation efficiency, and/or onto low-mass BHs. While current LLAGN statistics are too poor to draw firm conclusions, dust and gas may obscure a large fraction of LLAGN. The eROSITA-ART all-sky survey will detect hundreds of LLAGN (depending on their actual space density) with X-ray luminosities  $10^{39}$ – $10^{41}$  erg  $s^{-1}$  within several tens of Mpc, thus enabling a quantitative study of the local population of LLAGN.

## 2.4. Combining with eROSITA Science

In the 0.5–2.0 keV band, eROSITA is expected to detect several million AGN during the all-sky survey. In that ART-XC and eROSITA employ identical CCD detectors with excellent energy resolution, we shall reliably stack images to accumulate average spectra of large numbers of AGN, even when detection by ART-XC alone is lacking. Stacking - co-adding images at many well-specified locations each containing a known source (detected by eROSITA or SDSS, for example) - has been used with some success for X-ray deep fields - e.g., from Chandra [8, 9, 10, 11] and XMM-Newton [12]. Where redshifts to individual sources can be determined, we shall stack the spectra of thousands of individual AGN to obtain high-quality average spectra as functions of distance and type (e.g., obscured or unobscured). The combined eROSITA-ART all-sky survey will therefore enable the systematic study of the X-ray spectral-flux distributions of different types of AGNs over a broad energy range from below 1 keV to few tens of keV in the AGN rest frame. By averaging over peculiarities of individual objects and increasing statistics, this analysis will lead to new insights into the physics and geometry of accretion flows onto massive black holes that may be inferred from the spectrum, luminosity, and redshift.

## 2.5. Pointed Observations

During SRG pointed observations approximately 600 selected targets will be observed. ART-XC will extend the spectral coverage for observations of the brighter sources up to about 15 keV. For observations of thermal sources such as clusters of galaxies and supernova remnants, ART-XC will be used to search for non-thermal components that appear as a flattening of the continuum at high energies above the thermal emission. For non-thermal sources, ART's higher-energy response will improve measurements of the continuum slope and of the neutral and ionized iron-K equivalent widths. By detecting statistically significant numbers of photons at energies above the Fe-K complex, ART-XC will help to determine the shape of the continuum underlying these emission lines and thus provide a higher-fidelity measure of their strengths.

Another contribution from ART-XC during the pointed phase will be from its 3 “blank-field” images for each pointed observation. Assuming about 150 observations/year lasting  $\geq 0.1$  Ms, the “pointed” survey will cover approximately  $120 \text{ deg}^2$  ( $3 \times 18 \times 18 \text{ arcmin}^2$  fields,  $4.5 \text{ deg} - 6.5 \text{ deg}$  from the target, per pointed observation) to a deeper 2–10 keV sensitivity -  $7 \times 10^{-15} \text{ erg s}^{-1}$  - than the other SRG (ART-XC or eROSITA) surveys. Further, ART-XC uniquely obtains these data, in that all eROSITA modules are co-aligned and observing the target of the pointed-mode observation. This medium-deep survey will complement the SRG all-sky and polar surveys, as well as the deeper but narrower Chandra and XMM-Newton surveys.

For pointed observations of Galactic sources, the off-target fields will be used to build a census of the numerous nearby X-ray sources - including cataclysmic variables, isolated neutron stars, late-type flare stars, and high- and low-mass X-ray binaries. The good angular resolution of the ART-XC telescopes will be critical for source identifications at low Galactic latitudes.

Finally, the possibility exists that no other (2–10 keV) X-ray satellites will be operating during the SRG mission timeline. Thus, the responsibility of long-term monitoring of well-studied X-ray sources will fall to the SRG instruments including ART-XC. Any recurring transient or new source discovered (in any energy band) may also become an SRG target.

### 3. ART-XC DESCRIPTION

#### 3.1. General ART-XC design

The ART-XC instrument consists of 2 identical X-ray-telescope systems (Figure 1), each containing 4 mirror modules focused onto a single focal-plane CCD. To achieve this configuration, the mirror modules are symmetrically canted 3.2 deg to the central axis of the optical bench, optimizing performance for the mission’s 4-year scan phase. The CCD is partitioned into 4 quadrants with a simple cross-shaped baffle to prevent ghost imaging between the 4 modules for sources far off axis. Two mirror modules, one from each telescope system, are co-aligned with the spacecraft pointing axis to enable pointed observations. Table 3 summarizes the mirror configuration and the overall ART-XC instrument performance specifications.

Table 3: ART-XC mirror configuration and system performance

Number of Modules	8
Focal Length	2.7 m
Energy Range	2–11 keV
Number of Shells per Module	20
Outer Shell Diameter	184 mm
Inner Shell Diameter	93 mm
Shell Total Length	600 mm
Module field of view	$18 \text{ arcmin} \times 18 \text{ arcmin}$
System Effective Area for Pointed Observations	$220 \text{ cm}^2 @ 6.4 \text{ keV}$ (2 modules)
System Grasp for Survey	$60 \text{ deg}^2 \text{ cm}^2 @ 6.4 \text{ keV}$ (8 modules)

ART-XC is designed in collaboration between the Space Research Institute, Moscow (IKI), VNIIEF (Sarov, Russia), MPE (Germany), MSFC, USRA, SAO (all USA).

#### 3.2. Mirror system

The mirror fabrication will be made using an electroformed-nickel-replication technique that has been developed and employed over the past 15 years. In this process, thin nickel or nickel-alloy shells are electroformed onto figured and polished electroless-nickel-plated aluminum mandrels, from which they are later separated by differential thermal

contraction. The attraction of the ENR process for thin-shell X-ray mirrors is that the resulting optics are full shells of revolution and this makes them inherently stable with good figure control. This in turn offers the potential of good angular resolution.

A large number of mirror shells have been fabricated at MSFC using this technique, ranging in diameter from 2.5 cm, up to 0.5 m. These include over 30 ultra-thin shells (100  $\mu\text{m}$  thick) as part of a development program for a potential hard-X-ray telescope on the Constellation-X mission [13], and 96 replicated shells on board the MSFC HERO balloon payload [14]. While angular resolutions as low as 11 arcsec half-power diameters (HPD) have been achieved with individual shells, typical shells lie in the 13–15 arcsec HPD range and assembled modules around 20–28 arcsec HPD. Figure 5 shows a HERO module with  $\sim 10$  cm-diameter outer shells.

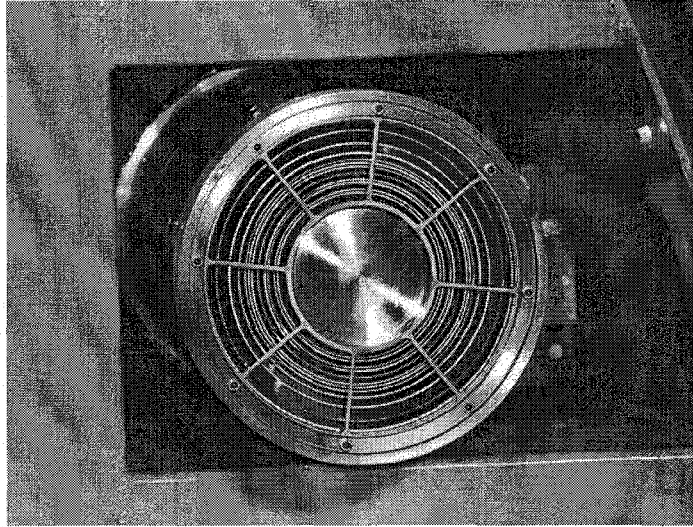


Figure 5: HERO mirror module, similar in design to the ART-XC modules

To meet the ART-XC science goals a grasp of  $>50 \text{ deg}^2 \text{ cm}^2$  and an effective area of  $>200 \text{ cm}^2$ , both at 6.5 keV, are required. We plan to achieve this through a configuration of 8 mirror modules focused on to 2 CCD focal planes. The mirror modules will be mounted on 2 optical benches with four modules and a single CCD each. The CCDs will be mechanically partitioned into quadrants, 1 per mirror module, to ensure that there is no ghost imaging from adjacent modules for sources far off axis. The arrangement is shown schematically in Figure 6.

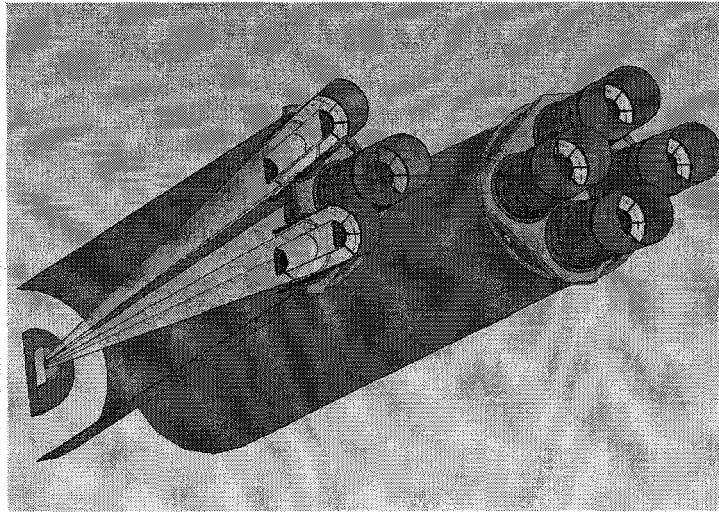


Figure 6. ART instrument configuration, sectioned (left) to show beam paths converging onto a single CCD

Each mirror module to be provided will consist of 20 nested electroformed nickel Wolter-1 shells as detailed in Table 4. The shells will be held in the modules with an 8-spoked spider on each end, similar to that shown in Figure 5. The spider material is a nickel alloy, K500 monel, chosen to closely match the thermal expansion coefficient (CTE) of the mirror shells. This ensures stability over a reasonable temperature range. Similarly, the mirror module housing is fabricated from stainless steel, which also has a CTE close to that of the shell material.

Table 4: ART-XC mirror configuration

Number of Modules	8
Focal Length	2.7 m
Energy Range	2-11 keV
Number of Shells per Module	20
Outer Shell Diameter	184 mm
Inner Shell Diameter	93 mm
Graze Angles	15 – 29 arcmin
Shell Thickness	300 $\mu$ m
Shell Segment Length	300 mm
Shell Total Length	600 mm
Shell Material	NiCo
Coating	Ir, 200 nm
Pre-Collimator Length	150 mm

### 3.3. Focal detector

Rapid readout is an important requirement for the focal plane system as in survey mode, the SRG spacecraft scan period can be as fast as 96 minutes. Thus, the scan rate across the sky is 225 (deg/hr = arcmin/min = arcsec/s) and so the 25 arcsec resolution element of the proposed mirror system is covered in approximately 0.1 sec. To avoid blurring,



therefore, the CCD must be read out in less than this time period. The eROSITA CCD, employed by ART-XC, will have a nominal integration time of 50 msec. This short time, and the relatively low fluxes per optics module, will also ensure that there will only be, at most, 1 photon hit per pixel.

In operation, each 384×384 pixel CCD is read into the frame store area in approximately 200 μs. This rapid transfer reduces out-of-time events, which can cause image smearing, to under 0.4%. After this, 3×128 channel CMOS Analog Multiplexing (CAMEX) readout chips transfer the data for digitizing within approximately 5 ms. Signal processing is performed within a detector main computer that performs pedestal subtractions and applies pixel noise thresholds according to stored maps. From here, data are sent to a controller that provides formatting for the spacecraft telemetry stream.

The expected energy resolution of the CCDs, operating at 20 frames/sec and a temperature of -80°C, is around 140 eV FWHM at 6 keV and ~80 eV FWHM at 2 keV. To avoid degradation of this performance over the ~7 year mission lifetime, substantial shielding (1 cm of copper) will be employed to reduce radiation doses should the non-equatorial or L2 orbit be selected. An inner graded shield consisting of B<sub>4</sub>C and Al<sub>2</sub>O<sub>3</sub> will be used inside this to attenuate copper fluorescent lines. It should be noted that, the above precautions aside, the pnCCD is relatively radiation hard, particularly against protons. The combination of this inherent hardness, plus the back illumination mode of operation, should mitigate the effects of focused low-energy protons.

The useful energy range of the detector system is set by the 100 nm aluminum entrance coating (a light filter) on the CCD at lower energies and by the transparency of the silicon at high energies. Over the energy range from 0.3 to 11 keV, the CCD will have greater than 90% quantum efficiency.

For ART, the configuration we are proposing will have 4 telescope modules focused on to 1 CCD, each module occupying ¼ of the total area. A mechanical baffle will prevent the fields of view of each of the 4 modules from overlapping to avoid ghost images that could cause ambiguities in source locations. As each CCD has an active area of ~29 mm × 29 mm, each 2.7-m focal length module will have a field of view of 18 arcmin × 18 arcmin.

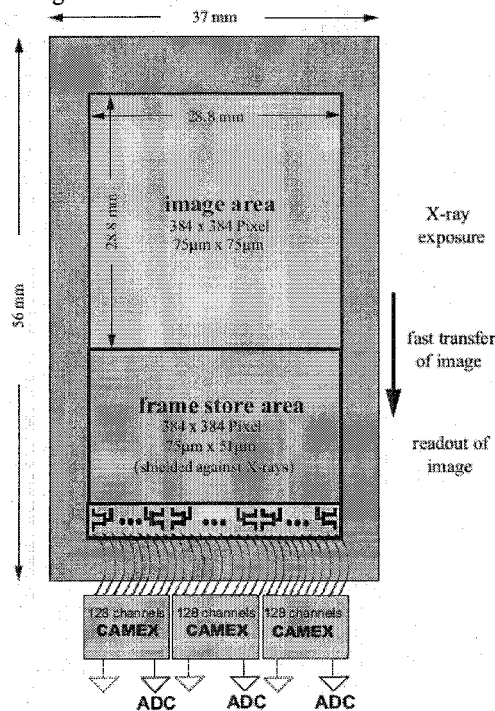


Figure 7: CCD data flow

### 3.4. Expected Sensitivity

We modeled the response of the ART instrument for the optics configuration and the detector described in previous sections. In addition, we assumed a 92%-bulk iridium optical coating, a thermal shield of 30-nm aluminum on 6- $\mu\text{m}$  Mylar at each end of a mirror module, and 8% geometric obstruction.

Figure 8 shows the calculated on-axis effective area  $A_{\text{eff}}(0)$  (per co-aligned module pair) and the system effective grasp  $G_{\text{eff}}$  (all 8 modules combined). In calculating the grasp, we use an 18 arcmin  $\times$  18 arcmin ( $0.09 \text{ deg}^2$ ) detector field of view - i.e.,  $1/4$  of a 2.88-cm<sup>2</sup> CCD at 270-cm focal length. The effective grasp, which is the field-averaged effective area times the solid-angle of the detector, is the most appropriate parameter for characterizing a survey instrument. In that the detector half field of view (9 arcmin) is substantially less than the mean grazing angles (15 arcmin – 29 arcmin) of the optics, the effects of vignetting and off-axis blur (oblique spherical aberration and coma) are reasonably small (but not negligible). In particular, for each module, the field-averaged effective area is about 70% of its on-axis value and the field-averaged RMS blur due to off-axis aberrations is  $<10$  arcsec - small when added in quadrature with the RMS blur due to mirror fabrication errors.

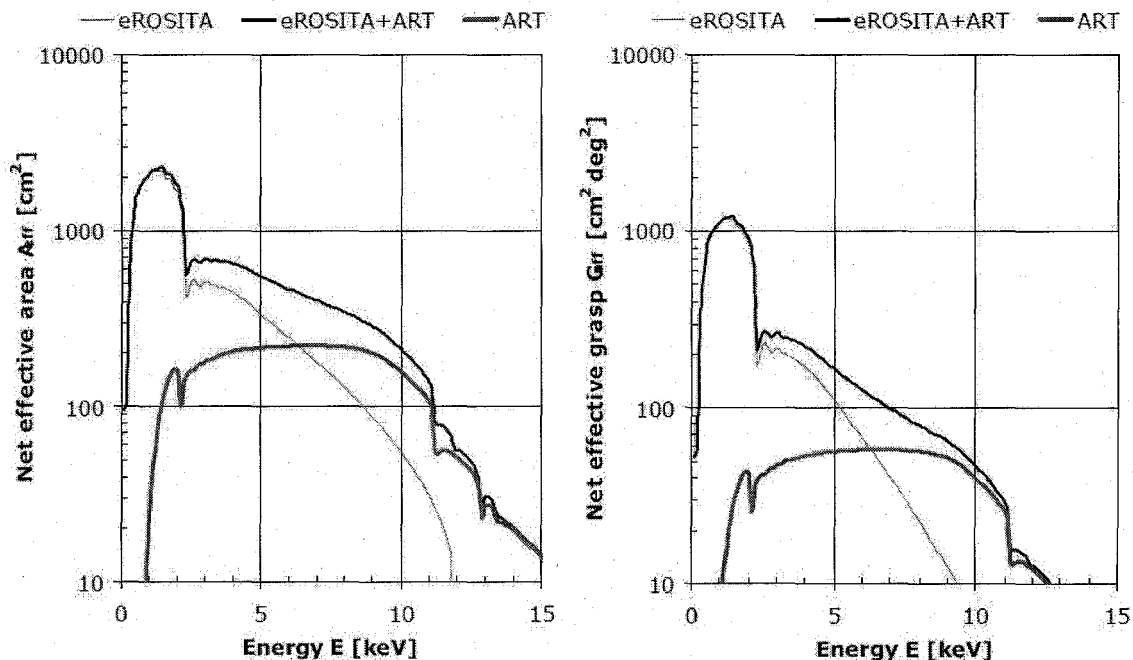


Figure 8: Comparison of ART (thick blue line) and eROSITA (thin red line) on-axis effective area  $A_{\text{eff}}(0)$  (left) and effective system grasp  $G_{\text{eff}}$  (right). ART doubles the response to iron-K emission and extends the energy range of SRG imaging to above 11 keV for detecting some heavily obscured AGN.

In addition to the ART response, Figure 8 shows the response of the eROSITA instrument and the response of eROSITA+ART combined. Note that eROSITA, which employs 7 co-aligned mirror modules (160-cm focal length) each with one full CCD, has a much softer response and larger field of view than does ART. In the iron-K band (near 6.5 keV), the responses of eROSITA and ART are comparable. Thus, in this astrophysically important spectral band and above, ART-XC contributes significantly to the SRG mission.

For any direction  $n$ , the effective exposure -  $X_n = t_n \langle A_{\text{eff}} \rangle_n$ , with  $t_n$  the time that direction is in the detector's field of view  $\Omega_{\text{det}}$  and  $\langle A_{\text{eff}} \rangle$  the average effective area over that time - determines the sensitivity of the observation for detecting imaged photons. Due to short exposure times and low background rates, the SRG surveys are all photon limited, thus the sensitivity depends upon the Poisson statistics of the imaged photons alone. Given  $X_n$  and specifying a minimum number of photons for detection, one can then calculate the sensitivity for various source spectra after

convolving the source number spectrum with the effective exposure - i.e., with the field-averaged effective area times the time a given direction is in the detector's field of view.

For our sensitivity calculations, we use a typical AGN spectrum with a photon power-law index of 1.9. In order to investigate the sensitivity to obscured AGN, we also consider the dependence upon column density  $N_H$  of detected photons for absorbed power-law spectra. From these sensitivity calculations, the  $\log N - \log S$  relation of Moretti et. al. [15], and the distribution of intrinsic column densities in a simple unified AGN model [16], we estimate the total number of AGN detected in a survey (Table 1) and the number detected as a function of intrinsic column (Table 2 and Figure 3).

#### 4. SUMMARY

The primary science objectives of the SRG ART-XC instrument are to enhance the sensitivity of an all-sky survey and pointed observations at and above the critical iron-K region and to enable the X-ray detection of some heavily obscured cosmic sources—especially local Active Galactic Nuclei (AGN). We have optimized the design of the ART instrument to achieve these science objectives. The sensitivity of the ART-XC system for 4 years of survey will be better than  $10^{-12}$  erg s $^{-1}$  cm $^{-2}$  over the 4–12 keV energy band. This will allow the ART-XC instrument to discover several thousand new AGNs.

#### REFERENCES

- [1] Daddi, E.; et al., “Multiwavelength Study of Massive Galaxies at  $z \sim 2$ . II. Widespread Compton-thick Active Galactic Nuclei and the Concurrent Growth of Black Holes and Bulges”, *ApJ*, 670, 173–189 (2007)
- [2] Steffen, A. T.; Brandt, W. N.; Alexander, D. M.; Gallagher, S. C.; & Lehmer, B. D., “Chandra Stacking Constraints on the Contribution of 24  $\mu$ m Spitzer Sources to the Unresolved Cosmic X-Ray Background”, *ApJL*, 667, L25–L28 (2007)
- [3] Brandt, W. N.; & Hasinger, G., “Deep Extragalactic X-Ray Surveys”, *ARA&A*, 43, 827–859 (2005)
- [4] Moretti, A.; Campana, S.; Lazzati, D.; & Tagliaferri, G., “The Resolved Fraction of the Cosmic X-Ray Background”, *ApJ*, 588, 696–703 (2003)
- [5] Barger, A. J.; Cowie, L. L.; Mushotzky, R. F.; Yang, Y.; Wang, W.-H.; & Steffen, A. T.; Capak, P., “The Cosmic Evolution of Hard X-Ray-selected Active Galactic Nuclei”, *AJ*, 129, 578–609 (2005)
- [6] Treister, E.; & Urry, C. M., “The Evolution of Obscuration in Active Galactic Nuclei”, *ApJL*, 652, L79–L82 (2006)
- [7] Ho, L. C.; Filippenko, A. V.; & Sargent, W. L. W., “A Search for “Dwarf” Seyfert Nuclei. V. Demographics of Nuclear Activity in Nearby Galaxies”, 487, 568–578 (1997)
- [8] Brusa, M.; Gilli, R.; & Comastri, A., “The Iron Line Background”, *ApJL*, 621, L5–L8 (2005)
- [9] Civano, F.; Comastri, A.; & Brusa, M., “X-ray spectral analysis of optically faint sources in the Chandra deep fields”, *MNRAS*, 358, 693–704 (2005)
- [10] Worsley, M. A.; Fabian, A. C.; Bauer, F. E.; Alexander, D. M.; Brandt, W. N.; & Lehmer, B. D., “Can the unresolved X-ray background be explained by the emission from the optically-detected faint galaxies of the GOODS project?”, *MNRAS*, 368, 1735–1741 (2006)
- [11] Lehmer, B. D.; Brandt, W. N.; Alexander, D. M.; Bell, E. F.; McIntosh, D. H.; Bauer, F. E.; Hasinger, G.; Mainieri, V.; Miyaji, T.; Schneider, D. P.; & Steffen, A. T., “The X-Ray Evolution of Early-Type Galaxies in the Extended Chandra Deep Field-South”, *ApJ*, 657, 681–699 (2007)
- [12] Tajer, M.; et al., “Obscured and unobscured AGN populations in a hard-X-ray selected sample of the XMDS survey”, *A&A*, 467, 73–91 (2007)
- [13] Ramsey, B and Gorenstein, P., *SPIE* 6688-40 (2007)
- [14] Ramsey, B.D., *Exp. Astron.* 20(1), 85 (2006)
- [15] Moretti, A.; Campana, S.; Lazzati, D.; & Tagliaferri, G., “The Resolved Fraction of the Cosmic X-Ray Background”, *ApJ*, 588, 696–703 (2003)
- [16] Treister, E.; & Urry, C. M., “Active Galactic Nuclei Unification and the X-Ray Background”, *ApJ*, 630, 115–121 (2005)

# SDMetrics Entry - Presentations

Title: ART-XC: a medium-energy X-ray telescope system for the Spectrum-R-Gamma mission

Presenters: V. Arefiev, M. Pavlinski, I. Lapshov, A. Tkachenko, S. Sazonov, M. Revnivitsev, N. Semena, M. Buntov, A. Vikhlinin, M. V. Gubarev, S. L. O'Dell, B. D. Ramsey, S. E. Romaine, D. A. Swartz, M. C. Weisskopf, G. Hasinger, P. Predehl, S. Grigorovich, D. Litvin, N. Meidinger, L. W. Struder

Conference Name: SPIE Conference

Location: Marseille, France

Conference Start Date: 6/21/2008

Conference End Date: 6/29/2008

Date Presented:

Conference Proceedings to Follow: No

Organization: VP62